



Participation of surface bicarbonate, formate and methoxy species in the carbon dioxide methanation catalyzed by ZrO₂-supported Ni



Alfredo Solis-Garcia, Jose F. Louvier-Hernandez, Armando Almendarez-Camarillo, Juan C. Fierro-Gonzalez*

Departamento de Ingeniería Química, Instituto Tecnológico de Celaya, Av. Tecnológico y Antonio García Cubas s/n, Celaya, Guanajuato 38010, Mexico

ARTICLE INFO

Article history:

Received 17 February 2017

Received in revised form 26 May 2017

Accepted 20 June 2017

Available online 28 June 2017

Keywords:

Supported nickel

Carbon dioxide

Carbon dioxide methanation

Infrared spectroscopy

Mass spectrometry

ABSTRACT

ZrO₂-supported Ni samples were prepared by an impregnation method and tested as catalysts for CO₂ methanation. Infrared spectra recorded during catalysis show that CO₂ was initially adsorbed in the form of carbonate and bicarbonate species bonded to sites of the support. The data indicate that bicarbonates were hydrogenated to give surface formate species, which reacted with H₂ at increasing temperature and led to the formation of methane, as evidenced by changes in the mass spectral signal of methane in the effluent gases from a flow reactor/DRIFT cell. No surface carbonyls were observed during the reaction. Separate experiments in which the catalysts were tested for the hydrogenation of methanol and formic acid also show their activity towards methane formation. In both cases, surface methoxy species bonded to Lewis acid sites of ZrO₂ were identified. Our results indicate a bifunctional character of the ZrO₂-supported Ni catalysts for CO₂ methanation, with the CO₂ being activated on sites of the support and the role of Ni consisting on providing sites for hydrogen adsorption and dissociation.

© 2017 Elsevier B.V. All rights reserved.

1. Introduction

The use of fossil fuels in the last decades has led to the increase of the atmospheric concentration of carbon dioxide, a greenhouse compound associated with global warming and climate change. Although research has been conducted to find methods for the use of CO₂ as a carbon source in the synthesis of chemicals and fuels, the relatively high stability of the CO₂ molecule poses substantial challenges. Among the transformations that involve the use of CO₂ as a reagent, its reactions with H₂ are the most explored [1–11], and a myriad of compounds can be obtained from them, including methane [2,3], methanol [4,5], ethanol [6,7], dimethyl ether [8,9], formic acid [10,11], and other products [1].

The catalytic production of methane from CO₂ hydrogenation (CO₂ methanation) can be performed at atmospheric pressure and at temperatures lower than 400 °C, as opposed to other hydrogenation reactions, which are only achieved at relatively high pressures. The first report of CO₂ methanation dates back to as early as 1902 [12], when Sabatier encountered that pure nickel catalyzed the production of methane from CO₂. Since then, it has been found that

various metal oxide-supported metals (e.g., Ni, Rh, Ru and Pd) are catalytically active and selective for that reaction [13–20].

Although the CO₂ methanation appears to be a relatively simple reaction, involving small and simple molecules, details concerning its mechanism are still obscure. Specifically, there is an ongoing debate regarding the identity of reaction intermediates and the nature of the surface sites on which the reaction takes place on the catalysts. In general, two reaction routes have been proposed in the presence of supported nickel catalysts: (a) one in which CO is considered to be an intermediate [21–23], and (b) another in which it is suggested that CO₂ is transformed into methane without formation of CO in the process [13,14,24].

Fujita et al. [21] and Aziz et al. [23] investigated the CO₂ methanation catalyzed by Ni dispersed on Al₂O₃ and on mesostructured silica nanoparticles, respectively. In both cases, nickel carbonyls were observed under reaction conditions and the authors proposed that these species were involved in the reaction. In contrast, Aldana et al. [13] investigated the CO₂ methanation catalyzed by Ni supported on CeO₂-ZrO₂ and found no evidence of nickel carbonyl species. Instead, they suggested that CO₂ was adsorbed on the catalyst in the form carbonates and bicarbonates, which were subsequently reduced by H₂ to produce formate species. It was proposed that formate species were further hydrogenated to give methane through a route that might involve the participation of formaldehyde-type species as reaction intermediates. Pan et al.

* Corresponding author.

E-mail address: jcfierro@iqcelaya.itc.mx (J.C. Fierro-Gonzalez).

[14] proposed a similar reaction route for the CO₂ methanation on Ni/Ce_{0.5}Zr_{0.5}O₂ catalysts, but suggested that formaldehyde-type species were not involved. Thus, the identity of the reaction intermediates is still a mystery, with various proposals arising from different samples. Moreover, the sequence of the transformations of CO₂ to the various surface species that ultimately lead to the formation of methane is still elusive.

Here we report the combined use of infrared (IR) spectroscopy and mass spectrometry for the characterization of ZrO₂-supported nickel samples as they functioned as catalysts for CO₂ methanation. Our data suggest that nickel carbonyls are not involved in the catalysis at the conditions of our experiments. To investigate the possible participation of formate and methoxy species in the reaction, we also studied the separate hydrogenations of formic acid and methanol on the samples. Our results allowed us to propose a reaction route that involves the transformation of bicarbonate species into formate and methoxy species, which ultimately lead to methane formation.

2. Experimental

2.1. Synthesis of ZrO₂-supported nickel samples

For the synthesis of ZrO₂, a precipitation method [25] was used. In the process, a 1 M aqueous solution of NH₄OH (Karal) was added dropwise at room temperature to a 0.3 M solution of ZrO(NO₃)₂ (Sigma-Aldrich) under constant stirring until the pH of the mixture reached a value of approximately 10.0. At that point, a white precipitate was formed, which was aged for 1 h and then it was filtered and washed with deionized water. Subsequently, the solid was dried overnight at 100 °C and then it was calcined in air at 500 °C for 5 h.

ZrO₂-supported nickel samples were prepared by an impregnation method [14], in which the support was brought in contact with a solution of Ni(NO₃)₂·6H₂O (Sigma-Aldrich) at room temperature. The concentration of the solution was calculated to obtain samples with a nickel loading of 1% wt. The impregnated samples were dried at 100 °C for 5 h, and then calcined in static air at 500 °C for 5 h.

2.2. Characterization of ZrO₂ and ZrO₂-supported Ni samples

2.2.1. Transmission electron microscopy (TEM)

TEM images of the supported Ni sample that had been treated with H₂ at 600 °C were recorded on a JEOL JEM-1010 transmission electron microscope. Prior to the measurements, the powder samples were dispersed in ethanol using an ultrasound cleaning bath. Then, they were placed on the copper grid and the solvent was evaporated at room temperature. The images were acquired at 80 kV.

2.2.2. X-ray diffraction characterization

The zirconia and zirconia-supported Ni samples were characterized by X-ray diffraction with an EasyX600 diffractometer (TNX X-ray Technologies) equipped with a constant potential X-ray generator operating at 25 kV/15 mA with a Cu target ($\lambda(\text{CuK}\alpha_1) = 0.1540598 \text{ nm}$). The scanning was performed with a step of 0.021° at 0.1 s per step in a range of 2θ between 20 and 90°.

2.2.3. X-ray absorption spectroscopy

X-ray absorption near edge structure (XANES) spectra at the Ni K edge were measured at the X-ray beamline D04B-XAFS1 at the Brazilian Synchrotron Light National Laboratory. For the experiments, self-supporting wafers of the ZrO₂-supported Ni samples were placed in a stainless steel holder inside a quartz cell that was previously aligned in the beamline. XANES spectra were recorded in transmission mode for the initially prepared samples and for

samples that had been exposed to a flowing mixture of H₂ (20%) in balance He at 600 °C for 30 min. The beamline was equipped with a Si (111) monochromator and the XANES spectra were calibrated by measuring the spectra of a Ni foil in transmission mode. The software Athena [26] was used for the data reduction and analysis. The data were normalized by dividing the absorption intensity by the height of the absorption edge, which is represented as the inflection point of the first absorption peak at nearly 8333 eV.

2.2.4. Infrared spectroscopy characterization of supported nickel catalysts during CO₂ methanation

IR spectra were recorded with a Nicolet FTIR 6700 spectrometer equipped with a HarrickTM reaction chamber in the diffuse reflectance Fourier transform (DRIFT) mode with a wavenumber resolution of $\pm 4 \text{ cm}^{-1}$ in the range between 4000 and 400 cm^{-1} . For the measurements, samples of the bare support and ZrO₂-supported nickel were loaded into the cell, which was closed and isolated with two standard three-way vacuum valves. Prior to the experiments the samples were reduced by means of a treatment in flowing H₂ (80 mL min⁻¹) at 600 °C for 40 min and then they were cooled to room temperature in flowing H₂. For the CO₂ methanation experiments, each sample was exposed to a flowing mixture consisting of H₂ (60 mL min⁻¹) and CO₂ (15 mL min⁻¹) as the temperature of the flow reactor/DRIFT cell was increased from room temperature to 400 °C at a rate of 5 °C min⁻¹. We warn that the actual temperature at the surface of the sample might be lower than that at the rest of the flow reactor/DRIFT cell, as Li et al. have reported [27]. Each reported spectrum corresponds to 150 scans and KBr powder was used as a reference material.

In other experiments, the samples (after reduction in flowing H₂) were treated with flowing mixtures of methanol/H₂ or formic acid/H₂. In each case, the reactant mixture was fed to the flow reactor/DRIFT cell by flowing H₂ (50 mL min⁻¹) through a saturator that contained either methanol or formic acid at room temperature. Simultaneously, IR spectra were recorded as the temperature of the flow reactor/DRIFT cell was increased from room temperature to 400 °C at a rate of 5 °C min⁻¹.

2.2.5. Mass spectra characterizing the effluent gases from the flow reactor/DRIFT cell

Concomitant with the IR measurements, mass spectra of the effluent gases from the flow reactor/DRIFT cell were recorded with an on-line Pfeiffer OmniStarTM mass spectrometer. During the experiments, the changes in the signal intensities of the main fragments of methane ($m/e = 16, 15, 14, 13$ and 12), water ($m/e = 18, 17$ and 16), methanol ($m/e = 32, 31, 29$, and 15), formic acid ($m/e = 46, 45, 44, 29$ and 28), carbon monoxide ($m/e = 29, 28, 16$ and 12) and carbon dioxide ($m/e = 44, 28, 16$ and 12) were monitored as a function of the temperature of the samples.

3. Results and discussion

3.1. Evidence of nickel nanoparticles on ZrO₂

Fig. 1 shows a comparison between the X-ray diffraction (XRD) patterns of a zirconia-supported Ni sample (before and after reduction in flowing H₂ at 600 °C) and those of ZrO₂ in monoclinic and tetragonal phases. The XRD patterns of our supported Ni samples include peaks at 28 and 31.3°, which are also present in the XRD pattern of monoclinic ZrO₂, together with a peak at 30°, attributed to the (101) reflection of tetragonal ZrO₂. Thus, it is concluded that our samples contained mixtures of ZrO₂ in the tetragonal and monoclinic phases, as others have also observed [25,28]. No diffraction peaks of NiO or Ni were observed, indicating that the supported nickel species were dispersed well on the surface of the ZrO₂ support.

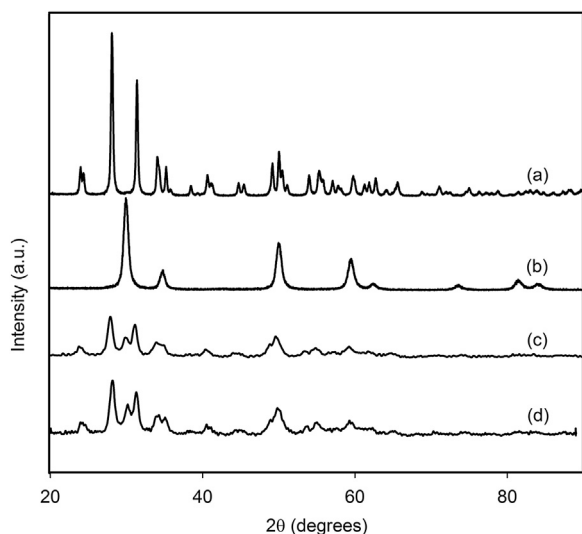


Fig. 1. X-ray diffraction patterns of (a) m-ZrO₂ [26], (b) t-ZrO₂ [26], and the ZrO₂-supported Ni sample (c) before and (d) after being treated in flowing H₂ at 600 °C.

Fig. 2 shows XANES spectra of the supported Ni sample before and after reduction in flowing H₂. The data indicate that the initially prepared sample contained predominantly Ni²⁺, as evidenced by the presence of features that resemble those of XANES spectra of the Ni(NO₃)₂ precursor (Fig. 2). After the treatment in flowing H₂, the nickel was reduced to Ni⁰, as evidenced by the disappearance of the features characteristic of Ni²⁺ and the appearance of features that resemble those observed in XANES spectra of a Ni foil (Fig. 2). TEM images characterizing the sample after the H₂ treatment show the presence of Ni particles with an average diameter of approximately 11 nm (Supplementary data).

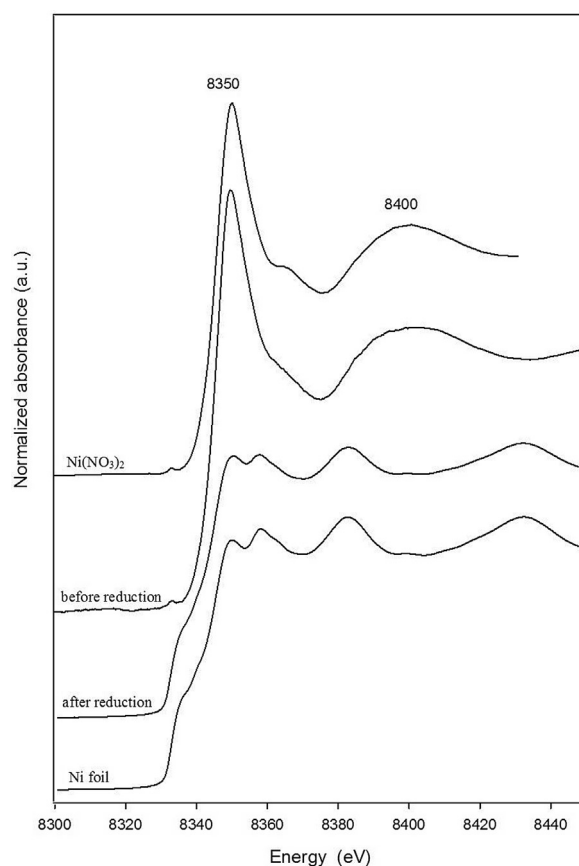


Fig. 2. Comparison between XANES spectra of Ni(NO₃)₂ and a Ni foil with those characterizing a sample of ZrO₂-supported Ni before and after reduction in flowing H₂ at 600 °C for 30 min.

3.2. CO₂ methanation catalyzed by ZrO₂-supported nickel catalysts

Mass spectra of the effluent gases from the flow reactor/DRIFT cell recorded as samples of ZrO₂ and ZrO₂-supported Ni (after reduction in H₂) were treated in a flowing mixture of CO₂ and H₂ at increasing temperature are shown in Fig. 3. The data show the onset of methane and water formation in the presence of the supported Ni sample at approximately 250 °C, as evidenced by the increase in the intensities of the signals of the mass fragments at *m/e* = 15 and 18, respectively (Fig. 3A). In contrast, when the same experiment was done in the presence of the bare ZrO₂ support, no methane formation was observed (Fig. 3B). Thus, it is concluded that Ni was necessary for the transformation of CO₂ into methane on the sup-

ported Ni sample. To test whether the formation of methane was catalytic, an experiment was performed by treating a sample of ZrO₂-supported Ni in a flowing mixture of CO₂ and H₂ at 300 °C. The results (Supplementary data) show that methane formation reached a steady state after approximately 20 min time on stream and the calculated CO₂ conversion was estimated to be 21%.

Mass spectra of the effluent gases measured as the bare ZrO₂ support was treated with the flowing CO₂/H₂ mixture show the formation of water at temperatures above 270 °C (Fig. 3B). A possible explanation for this observation is a reaction between surface-derived CO₂ species adsorbed on ZrO₂ and H₂. This possibility is addressed in detail in the following section.

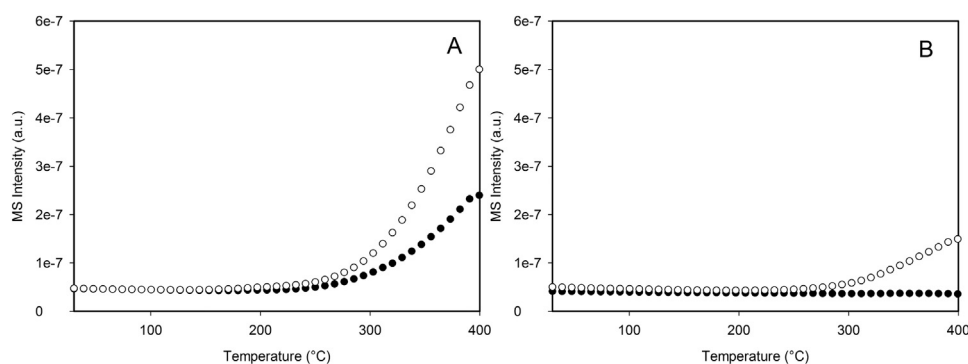


Fig. 3. Changes in the signal intensities of the mass fragments of CH₄ (●) and H₂O (○) in mass spectra of the effluent gases from the flow reactor/DRIFT cell as samples of (A) ZrO₂-supported Ni and (B) the bare support were treated in the flowing reactive mixture of CO₂ and H₂ at increasing temperatures.

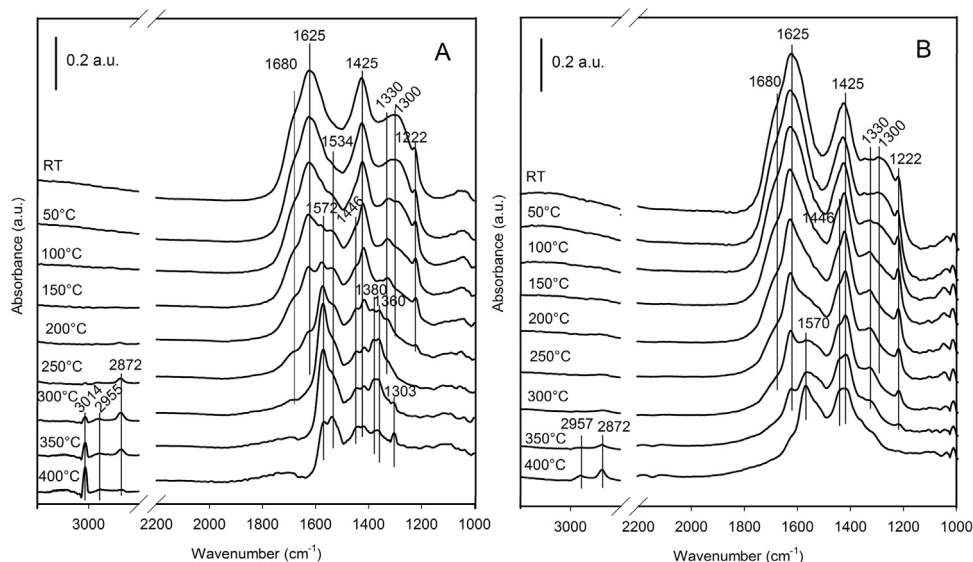


Fig. 4. IR spectra characterizing (A) the ZrO₂-supported Ni sample and (B) the bare support as they were treated in a flowing mixture of CO₂ and H₂ at increasing temperature.

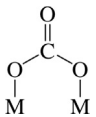
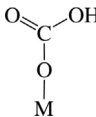
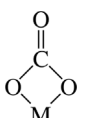
3.3. Surface species formed during CO₂ methanation catalyzed by ZrO₂-supported nickel catalysts

IR spectra characterizing samples of ZrO₂ and ZrO₂-supported Ni as they were treated in the flowing reactive mixture of CO₂ and H₂ at increasing temperature are shown in Fig. 4. The data show that admission of the reactive mixture at room temperature led to the appearance of the same bands in spectra of both samples at 1625, 1425, 1300 cm⁻¹ and 1222 cm⁻¹, together with a small shoulder at approximately 1680 cm⁻¹. The shoulder at 1680 cm⁻¹ and the band 1300 cm⁻¹ can be assigned to the asymmetric and symmetric CO₃ stretching ($\nu_{a\text{CO}_3}$, $\nu_{s\text{CO}_3}$) vibration modes of bridged carbonates on the surface of ZrO₂, respectively [29]. Similarly, the bands at 1625, 1425 and 1222 cm⁻¹ might be assigned to vibrations of surface bicarbonate species [30,31]. As the temperature increased to approximately 100 °C, these bands became more resolved and a new band could be distinguished in spectra of both samples at 1330 cm⁻¹. This band is attributed to the $\nu_s(\text{CO}_3)$ vibration mode of bidentate carbonate species [30–32]. A summary of the assignments of the various bands, based on the observation of similar

bands during the reactive adsorption of CO₂ on ZrO₂ [30,31], CeO₂ [30] and Ga₂O₃ [29], is shown in Table 1.

As the temperature increased above 100 °C, differences in the IR spectra of both samples were evident. Spectra of the bare support (Fig. 4B) show that when the temperature had reached approximately 300 °C, a band appeared at 1570 cm⁻¹. This band became more resolved as the temperature increased to 350 °C, at which point small bands appeared in the C–H stretching (ν_{CH}) region at 2957 and 2872 cm⁻¹ (Fig. 4B). Busca et al. [33] observed the appearance of similar bands (at 1570, 2965 and 2865 cm⁻¹) when they investigated the adsorption of formic acid on ZrO₂ and assigned them to surface formate species. Therefore, we attribute the bands at 1570, 2957 and 2872 cm⁻¹ to the $\nu_a(\text{CO}_2)$, $\nu_a(\text{CO}_2) + \delta(\text{CH})$ and $\nu(\text{CH})$ vibration modes of surface formate species on ZrO₂ [34]. At higher temperatures, the intensities of the bands assigned to surface formate species increased as those of the other surface species (carbonates and bicarbonates) decreased (Fig. 4B). Therefore, our results indicate that part of the CO₂-derived surface species initially present on the sample (i.e., carbonates and bicarbonates) were transformed into surface formate species on the ZrO₂ surface at approximately 300 °C. This transformation might have involved

Table 1
Frequencies (cm⁻¹) and assignments of observed IR bands of carbonate and bicarbonate surface species formed as the supported Ni sample and the bare support were treated in a flowing mixture of CO₂ and H₂.

| Sample | | Assignment | Surface species | Refs. |
|---------------------|------------------|----------------------|--|---------|
| Ni/ZrO ₂ | ZrO ₂ | | | |
| 1680 | 1680 | $\nu_a(\text{CO}_3)$ |  | [29] |
| 1300 | 1300 | $\nu_s(\text{CO}_3)$ | | |
| 1625 | 1625 | $\nu_a(\text{CO}_3)$ |  | [30,31] |
| 1425 | 1425 | $\nu_s(\text{CO}_3)$ | | |
| 1222 | 1222 | $\delta(\text{OH})$ | | |
| 1534 | 1330 | $\nu_a(\text{CO}_3)$ |  | [30,31] |
| 1330 | | $\nu_s(\text{CO}_3)$ | | |

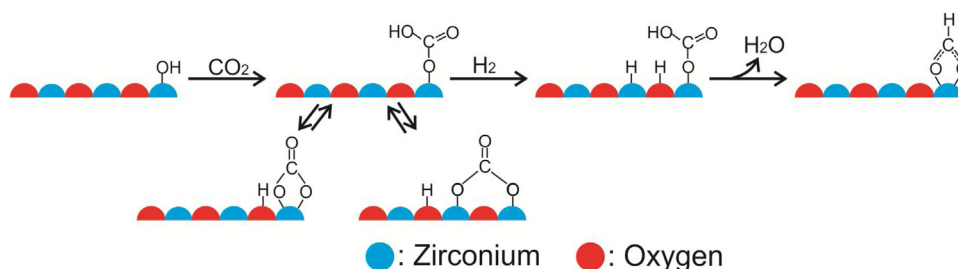


Fig. 5. Schematic representation of the reaction between bicarbonate species on ZrO₂ with H₂ to give surface formate species.

the reaction of bicarbonates with hydrogen atoms that resulted from the H₂ dissociation on the support at increasing temperature. Indeed, it has been reported [38] that H₂ is dissociated on ZrO₂ to give Zr–H and Zr–OH species. The reaction between surface bicarbonate species and dissociated hydrogen on ZrO₂ to give formate species is schematized in Fig. 5. Water is formed in the process, which is consistent with mass spectra of the effluent gases from the flow reactor/DRIFT cell showing an increase in the intensity of the mass fragment at $m/e = 18$ (Fig. 3B).

When the experiment was done in the presence of the supported Ni sample, the changes in the IR spectra (Fig. 4A) occurred at lower temperatures than in the presence of the bare support. Specifically, the band at 1572 cm^{−1}, assigned to the $\nu_a(\text{CO}_2)$ vibration mode of bidentate formate species, was observed at approximately 150 °C (Fig. 4A) [33]. When the temperature reached approximately 250 °C, two bands appeared at 1380 and 1360 cm^{−1}. These bands are assigned to $\delta(\text{CH})$ and $\nu_s(\text{CO}_2)$ of formate species doubly bonded to Zr⁴⁺ sites [33]. Spectra in the ν_{CH} region bolster the assignments of the bands at 1572, 1380 and 1360 cm^{−1} to formate species, showing the appearance of bands at 2955 and 2872 cm^{−1}, assigned to the $\nu_a(\text{CO}_2) + \delta(\text{CH})$ and $\nu(\text{CH})$ vibration modes of surface bidentate formate species (Fig. 4A) [33,39]. It is noted that the bands characteristic of $\nu_a(\text{CO}_2) + \delta(\text{CH})$, $\nu(\text{CH})$ and $\nu_a(\text{CO}_2)$ vibration modes of formates were essentially the same in the spectra of the bare support and the supported Ni sample. Therefore, our data suggest that the formate species were bonded to sites of the support and not to the Ni particles on the catalyst. The observation of formate species at lower temperatures on the supported nickel sample might be explained by the fact that H₂ dissociation was facilitated by the presence of Ni.

Starting at approximately 300 °C and with increasing temperature, bands were observed at 3014 cm^{−1} and 1303 cm^{−1} (Fig. 4A). These bands are assigned to the $\nu(\text{CH})$ and $\delta(\text{CH})$ vibration modes of methane gas, respectively [40], in agreement with mass spectra of the effluent gases from the flow reactor/DRIFT cell showing methane formation (Fig. 3A) [41,42]. Appearance of these bands coincided well with the decrease in the intensity of the bands associated with formate species. Again, the formation of methane suggests that Ni particles favored the dissociation of H₂ to hydrogenate the surface formate species.

A correlation between the intensity of the band at 1572 cm^{−1} (assigned to the $\nu_a(\text{CO}_2)$ vibration mode of formate species) and the intensity of the mass fragment of methane in the effluent gases from the flow reactor/DRIFT cell is shown in Fig. 6. It is noted that the band at 1572 cm^{−1} appeared at approximately 150 °C and its intensity reached a maximum value at approximately 310 °C. This observation indicates that the concentration of formate species on the surface of the sample increased between those temperatures. At higher temperatures, the band decreased in intensity, coinciding with the rapid formation of methane, as evidenced by the sharp increase in the intensity of the mass spectral signal at $m/e = 15$ (Fig. 6). It is noted that the temperature at which the decrease in the intensity of the band of formate species was observed is not exactly

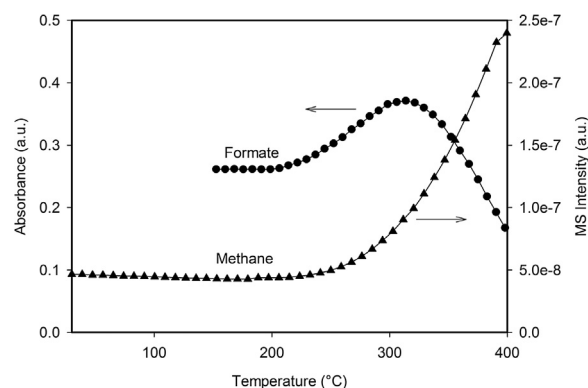


Fig. 6. Correlation between the intensity of the IR band at 1572 cm^{−1} (formate species) and the intensity of the mass fragment of methane in mass spectra of the effluent gases from the flow reactor/DRIFT cell as a ZrO₂-supported Ni sample was treated with the flowing reactive mixture of CO₂ and H₂ at increasing temperature.


the same as that at which the onset of methane formation occurred. The difference could be related to the existence of a temperature gradient between the surface of the sample (from which IR spectra were recorded) and the rest of the catalyst [27]. Nevertheless, the data suggest that formate surface species could be involved in the production of methane, although the specific way by which the formate species were converted to methane cannot be derived from spectra shown in Fig. 4. Our results are in agreement with previous reports [13,14,24,43], in which it has also been proposed that surface formate species could be involved in the CO₂ methanation catalyzed by supported nickel and other metals. However, there are other reports that propose the participation of Ni carbonyls in the reaction [21–23]. C–O stretching (ν_{CO}) bands of Ni carbonyls are expected to appear in the region between 1800 and 2100 cm^{−1}. We have no evidence of Ni carbonyls under our reaction conditions, as IR data of the supported Ni sample do not include bands at the ν_{CO} region (Fig. 4). Therefore, we conclude they were not involved in the catalysis. However, we do not rule out the possibility that they might participate in the CO₂ methanation catalyzed by other samples and at other reaction conditions.

It has been established that formate species are readily formed on the surfaces of metal oxides during the dissociative adsorption of formic acid. Thus, to gain more insight into the transformation of formate species, we investigated the hydrogenation of formic acid on the surface of our samples.

3.4. Formic acid hydrogenation catalyzed by ZrO₂-supported Ni

When a ZrO₂-supported Ni sample was treated in a flowing mixture of formic acid and H₂ at increasing temperatures, methane formation was observed at temperatures higher than approximately 250 °C, as evidenced by the increase in the intensity of the signal of its mass fragment at $m/e = 15$ (Fig. 7A). Concomitantly, the intensity of the mass fragment of H₂O, at $m/e = 18$, also increased.

Table 2
Frequencies (cm^{-1}) and assignments of observed IR bands of formate surface species formed on the supported Ni sample when it was treated in flowing mixtures of CO_2/H_2 , HCOOH/H_2 and $\text{CH}_3\text{OH}/\text{H}_2$.

| Ni/ZrO ₂ | | | Assignment | Species | Refs. |
|---------------------------------|----------------------|-----------------------------------|--|---|------------|
| CO ₂ /H ₂ | HCOOH/H ₂ | CH ₃ OH/H ₂ | | | |
| 2955 | 2958 | 2957 | $\nu_a(\text{CO}_2) + \delta(\text{CH})$ |  | [33,35–37] |
| 2872 | 2875 | 2875 | $\nu(\text{CH})$ | | |
| | | 1590 | $\nu_a(\text{CO}_2)$ Linear | | |
| 1572 | 1570 | 1573 | $\nu_a(\text{CO}_2)$ Bidentate | | |
| 1380 | 1380–1390 | 1380–1390 | $\delta(\text{CH})$ | | |
| 1360 | 1365 | 1354–1362 | $\nu_s(\text{CO}_2)$ | | |
| | 1790 | | $\nu(\text{C=O})$ | HCOOH _(ad) | [43,45] |
| | 1215 | | $\delta(\text{OH})$ | | |
| | 1120 | | $\nu(\text{CO})$ | | |
| | 1086 | | $\delta(\text{CH})$ | | |
| | 1750 | | $\nu(\text{CH})$ | HCOOH _(g) | [43,44] |
| | 1315 | | $\delta(\text{CH})$ | | |

Thus, it is concluded that the sample favored the hydrogenation of formic acid to give methane and H_2O . It is noted that the onset of methane formation during the hydrogenation of formic acid occurred at approximately the same temperature as that observed during the CO_2 methanation on our catalysts (Fig. 3A). The changes in the intensities of the mass fragments of CO ($m/e = 28$) and CO_2 ($m/e = 44$) as a function of temperature were also monitored during the experiment. The results show no evidence of CO formation, but a slight formation of CO_2 was observed at temperatures higher than approximately 230°C (Fig. 7A). These results indicate that part of the formic acid was oxidized on the surface of the sample.

IR spectra of the sample recorded during the treatment show the appearance of various bands upon admission of formic acid and H_2 to the flow reactor/DRIFT cell at room temperature (Fig. 7B). Specifically, the bands at 1790, 1215, 1120 and 1086 cm^{-1} are characteristic of gas-phase formic acid [44,45], whereas the intense band at 1750 cm^{-1} and the shoulder at 1315 cm^{-1} might be attributed to formic acid molecularly adsorbed on sites of the support [44,46]. A detailed description of the assignments of these bands is shown in Table 2. In turn, the bands at 1570, 1390 and 1365 cm^{-1} might be attributed to surface bidentate formate species bonded to the support [33] (Table 2). It is noted that the latter three bands were also observed during CO_2 methanation catalyzed by the supported Ni sample at 1572, 1380 and 1360 cm^{-1} , respectively (Fig. 4A). As the temperature increased, the bands corresponding to gas-phase and molecularly adsorbed formic acid decreased in intensity, and at approximately 300°C they had almost disappeared (Fig. 7B). At that point, the bands of formate species also started to decrease in intensity, with the concomitant appearance of bands at 1436, 1305, 1170 and 1090 cm^{-1} (Fig. 7B). The band at 1305 cm^{-1} is attributed to the $\delta(\text{CH})$ of methane [40], and its appearance coincides well with the onset of formation of methane, as observed by mass spectra of the effluent gases from the flow reactor/DRIFT cell (Fig. 7A). The data show that the increase in the formation of methane and the decrease in the integrated intensity of the band at 1570 cm^{-1} (assigned to formate species) occurred in approximately the same temperature range (Fig. 7A). Again, differences in temperatures could be attributed to a temperature gradient between the surface of the sample (from which IR spectra are recorded) and the rest of the catalyst [27]. It is noted that the decrease in the intensity of the band of formate species does not correlate with the formation of CO_2 . Thus, it is suggested that formate species participate in the hydrogenation of formic acid to give methane. Because formate

species bonded to sites of the ZrO_2 were also identified when the ZrO_2 -supported Ni sample was exposed to the flowing mixture of CO_2 and H_2 (Fig. 4), these results are consistent with the hypothesis that they participate in the CO_2 methanation catalyzed by our supported Ni samples. Again, the role of Ni might consist in providing sites for H_2 dissociation.

Assignment of the bands that appeared at approximately 300°C at 1436, 1170 and 1090 cm^{-1} is not straightforward. Others [47,48] have reported the presence of IR bands ranging from 1106 to 1163 cm^{-1} and from 1032 to 1083 cm^{-1} during the adsorption of methanol on metal oxides and have attributed them to the $\nu(\text{CO})$ vibration modes of linearly- and bridge-bonded methoxy species to Lewis acidic sites on metal oxides, respectively. Therefore, we assign the bands at 1170 and 1090 cm^{-1} to the $\nu(\text{CO})$ vibration modes of methoxy species bonded to ZrO_2 . This assignment is bolstered by the presence of the band at 1436 cm^{-1} , which could also be attributed to the $\delta(\text{CH}_3)$ vibration mode of surface methoxy species bonded to the support, as others have previously observed [49,50].

The appearance of bands characteristic of methoxy species under reaction conditions, together with the decrease in the intensities of bands of formate species and the formation of methane, could indicate that methoxy species participate in the hydrogenation of formic acid (and CO_2) to methane on the supported Ni sample.

3.5. Surface species derived from the reactions of methanol on ZrO_2 and ZrO_2 -supported Ni

It is known that methanol is adsorbed on metal oxides in the form of methoxy species [47,48]. Therefore, to explore the possible participation of methoxy species in the CO_2 methanation, an experiment was performed in which a ZrO_2 -supported Ni sample was treated with flowing methanol and H_2 at increasing temperature. Our hypothesis was that if surface methoxy species are indeed involved in the CO_2 methanation, our samples would also be active for the methanol hydrogenation to methane.

Mass spectra of the effluent gases recorded during the experiment are shown in Fig. 8A. The data show the onset of methane formation at approximately 220°C [51]. H_2O was also formed, but the behavior of its mass fragment ($m/e = 18$) was not exactly the same as that of methane (Fig. 8A). It has been proposed that the dissociative adsorption of methanol on metal oxides leads to the

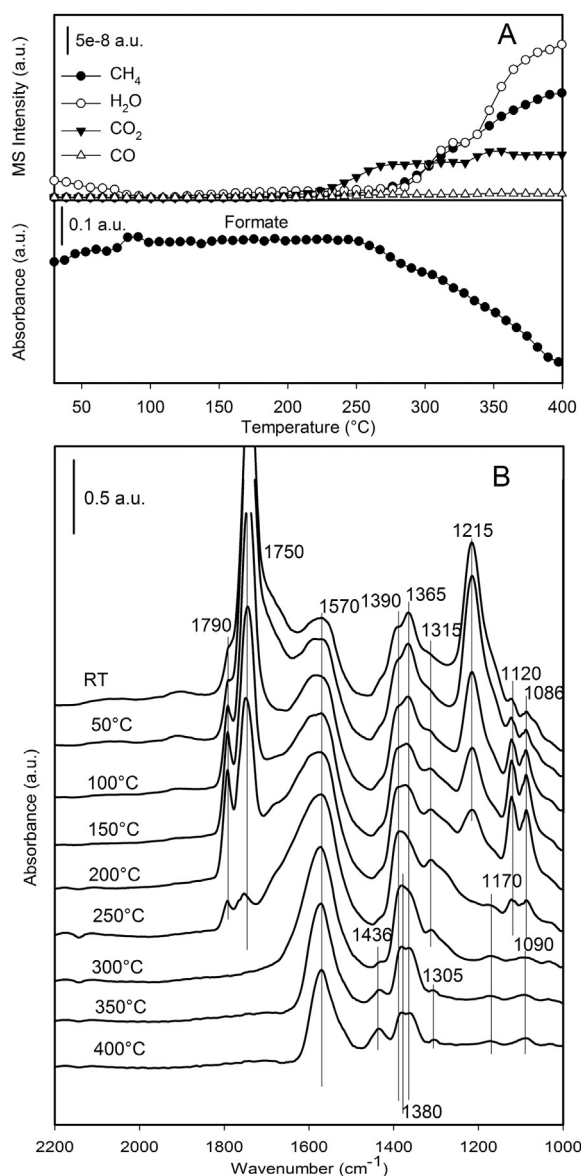


Fig. 7. (A) Correlation between the signal intensities of the mass fragments of CH₄ and H₂O in mass spectra of the effluent gases from the flow reactor/DRIFT cell and the intensity of the IR band at 1570 cm⁻¹ (formate species) as a ZrO₂-supported Ni sample was treated with the flowing mixture of formic acid and H₂ at increasing temperature. (B) IR spectra characterizing the ZrO₂-supported Ni sample during the formic acid hydrogenation at increasing temperature.

formation of methoxy species and water [52,53]. The latter could be desorbed at approximately 100 °C, which explains our observation of a first formation of water at approximately that temperature (Fig. 8A). In turn, the second formation of water occurred at temperatures that are similar to those at which methane was formed, thus indicating that methanol was hydrogenated to give methane and H₂O.

No CO was observed in the effluent gases from the flow reactor/DRIFT cell (Fig. 8A). However, a slight increase in the intensity of the mass fragment of CO₂ was observed at temperatures higher than 250 °C. Because the onset of CH₄ formation occurred at lower temperature it is proposed that CO₂ did not participate significantly in the reaction.

IR spectra characterizing the sample during the experiment are shown in Fig. 8B. It is observed that admission of methanol at room temperature led to the appearance of bands at 1160 and 1055 cm⁻¹. These bands are in the range of $\nu(\text{CO})$ vibration modes of linear

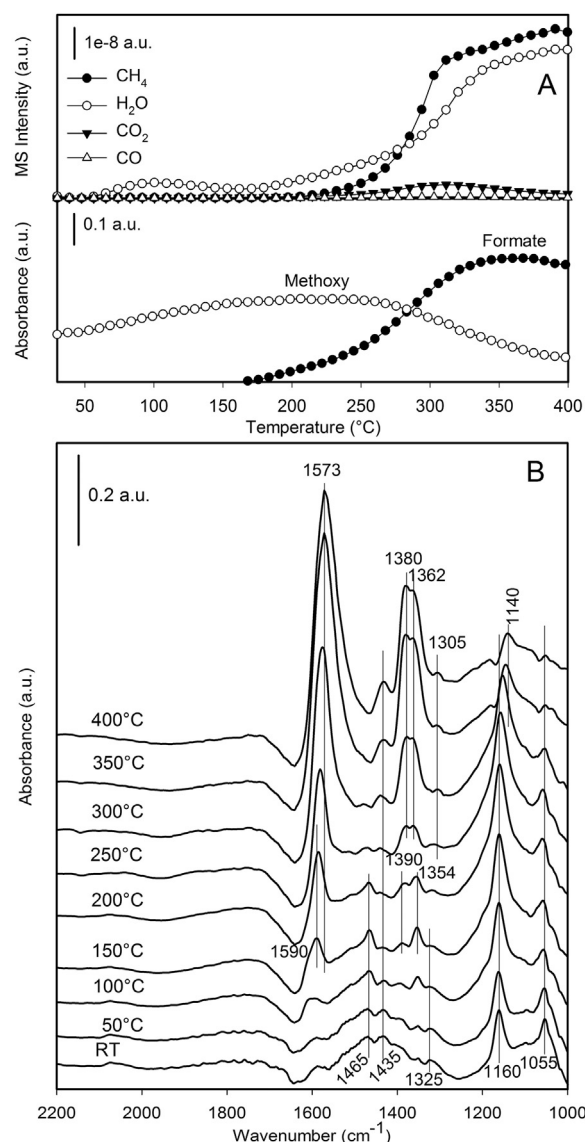


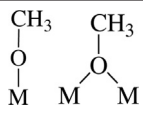
Fig. 8. (A) Correlation between the signal intensities of the mass fragments of CH₄ and H₂O in mass spectra of the effluent gases from the flow reactor/DRIFT cell and the intensities of the IR bands of formate and methoxy species as a ZrO₂-supported Ni sample was treated with the flowing mixture of methanol and H₂ at increasing temperature. (B) IR spectra characterizing the ZrO₂-supported Ni sample during the methanol hydrogenation at increasing temperature.

and bridged methoxy species bonded to Lewis acidic sites on metal oxides [47,48,54].

Admission of methanol to the flow reactor/DRIFT cell also led to the appearance of bands at 1325, 1435 and 1465 cm⁻¹, which could be assigned to the $\delta(\text{OH})$, $\delta_s(\text{CH}_3)$ and $\delta_a(\text{CH}_3)$ vibration modes of gas-phase methanol [55,56] (Table 3). At approximately 150 °C, bands appeared at 1590, 1390 and 1354 cm⁻¹. These bands can be assigned to $\nu_a(\text{CO}_2)$, $\delta(\text{CH})$ and $\nu_s(\text{CO}_2)$ vibration modes of monodentate formate species bonded to the support [33,34].

When the temperature increased to 200 °C the bands associated with methanol gas had almost disappeared, and the bands at 1160 and 1435 cm⁻¹ (assigned to $\nu(\text{CO})$) and $\delta(\text{CH}_3)$ of linear methoxy species had increased in intensity (Fig. 8B). Also, the bands associated with formate species increased in intensity, suggesting that even in the presence of H₂ part of the methoxy species were oxidized to formate species on the support. However, once the temperature reached 250 °C the bands of methoxy species started to decrease in intensity, with the simultaneous appearance of a band

Table 3
Frequencies (cm^{-1}) and assignments of observed IR bands of methoxy surface species formed on the supported Ni sample when it was treated in flowing mixtures of HCOOH/H_2 and $\text{CH}_3\text{OH}/\text{H}_2$.

| Ni/ZrO ₂ | | Assignment | Species | Refs. |
|----------------------|-----------------------------------|--------------------------|---|----------|
| HCOOH/H ₂ | CH ₃ OH/H ₂ | | | |
| | 2928 | $\nu_a(\text{CH}_3)$ |  | [46,47]* |
| | 2823 | $\nu_s(\text{CH}_3)$ | | |
| 1436 | 1435 | $\delta(\text{CH})$ | | |
| 1170 | 1160 | $\nu(\text{CO})$ Linear | | |
| 1090 | 1055 | $\nu(\text{CO})$ Bridged | | |
| | 146 | $\delta_a(\text{CH}_3)$ | $\text{CH}_3\text{OH}_{(\text{g})}$ | [54,55] |
| | 1435 | $\delta_s(\text{CH}_3)$ | | |
| | 1325 | $\delta(\text{OH})$ | | |

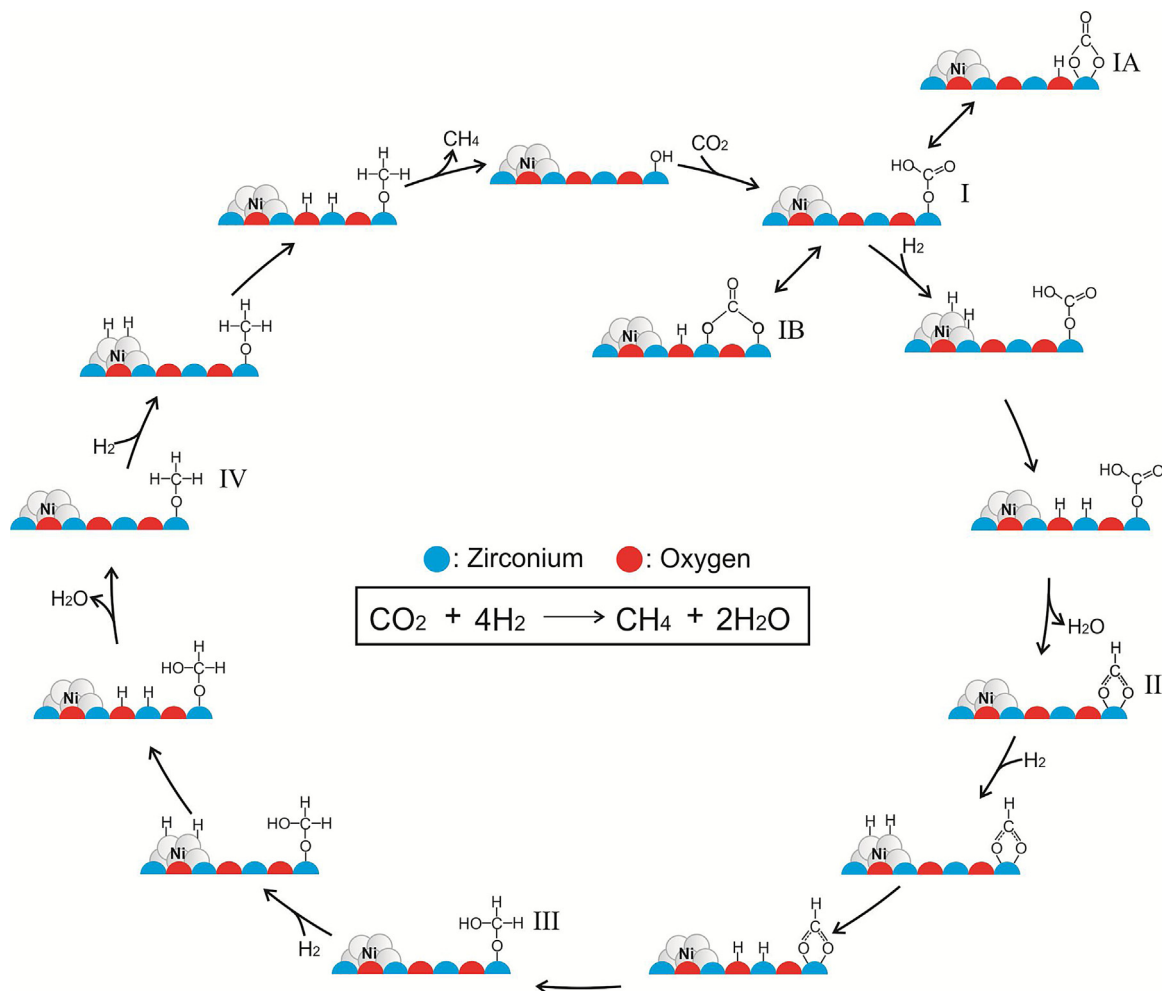


Fig. 9. Schematic representation of the CO_2 methanation on ZrO_2 -supported Ni catalysts.

a 1305 cm^{-1} , attributed to the $\delta(\text{CH})$ vibration mode of methane gas. At approximately the same temperature, mass spectra of the effluent gases from the flow reactor showed the rapid formation of methane (Fig. 8A). Therefore, the data suggest that methoxy species bonded to the support participated in the methanol hydrogenation to CH_4 . Because at 250°C H_2 could be dissociated on the surface of the Ni particles, it is proposed that H adatoms on Ni could hydrogenate methoxy species to give methane. In contrast, at lower temperatures the oxidation of methoxy species to formate species on the support was dominant, as evidenced by the accumulation of formate species. It is observed that the bands of surface formate species at 1590 and 1390 cm^{-1} shifted their frequencies

with increasing temperature to 1573 and 1380 cm^{-1} , respectively, indicating the conversion from linear to bidentate formate species [34].

To investigate whether the formation of methane was associated with the consumption of either formate or methoxy species, the changes in the intensities of the bands at 1570 – 1590 cm^{-1} (formate) and 1160 cm^{-1} (methoxy) were compared with the changes in the intensity of the mass fragment of methane (Fig. 8A). The data suggest that there is a good agreement between the consumption of methoxy species (evidenced by the decrease in the intensity of the band at 1160 cm^{-1}) and the formation of methane at temperatures higher than approximately 220°C . In contrast, formate

species accumulated on the surface of the sample even at temperatures higher than 300 °C. It is observed that the intensity of the band of formate species reached a maximum value at approximately 375 °C and it then remained nearly constant. From those observations we propose that methane formation was mainly due to the hydrogenation of methoxy species.

3.6. Participation of formate and methoxy species in the CO₂ methanation catalyzed by ZrO₂-supported Ni

Based on our results, we propose that the CO₂ methanation on ZrO₂-supported Ni catalysts occurs by a route that is schematically represented in Fig. 9. First, CO₂ reacts with surface OH groups of ZrO₂ to give bicarbonate species (Fig. 9, species I), as evidenced by the appearance of IR bands at 1625, 1425 and 1222 cm⁻¹ in the spectra of the samples at room temperature (Fig. 4A). The bicarbonate species can be reversibly converted into carbonate species (Fig. 9, species IA and IB), identified by IR bands at 1680 and 1300 cm⁻¹ for bridged carbonates and at 1534 and 1330 cm⁻¹ for bidentate carbonates. We stress that these CO₂-derived surface species were bonded to sites of the support, because the same bands were observed in IR spectra of the bare ZrO₂ and the supported Ni sample during CO₂ adsorption at room temperature (Fig. 4).

With increasing temperature, H₂ can be dissociated on the surface of Ni particles [23]. It has been proposed that H atoms on supported metals (resulting from H₂ dissociation) can migrate to reducible metal oxide supports by a spillover process [57,58]. Hoang et al. [58] proposed that hydrogen spillover leads to the formation of surface hydroxyl groups and metal–H species on the supports. We propose that bicarbonate species can react with both surface hydroxyl groups and Zr–H species to give formate species (bidentate) and water (Fig. 9, species II). The bidentate formate species are identified by IR spectra of the functioning catalyst showing bands at 2955, 2872, 1572, 1380 and 1360 cm⁻¹ (Fig. 4A). At temperatures higher than 250 °C the formate species are further hydrogenated, leading to the formation of methane.

Although IR spectra recorded during CO₂ hydrogenation did not allow the identification of intermediates between the formate species and methane, our IR spectra recorded during the separate hydrogenations of formic acid and methanol provide insight into the transformation of surface formate species on the supported Ni sample. From these data, we propose that more H₂ is dissociated on Ni particles to give surface OH groups and Zr–H species. We propose that both species could react with surface formates to give surface species III (Fig. 9). Pan et al. [14] observed very small bands at 1507 and 1340 cm⁻¹ during the methanation of CO₂ on Ni/Ce_{0.5}Zr_{0.5}O₂ catalysts and attributed them to δ(OH) and δ(CH) vibrations modes of species that are analogous to the species III in Fig. 9. Although we did not observe IR bands that might be unequivocally attributed to such species, theoretical studies at the DFT level have also suggested their formation during the CO₂ methanation on Ni single crystals [59]. Elimination of water from species III leads to the formation of methoxy species bonded to sites on the ZrO₂ support (Fig. 9, species IV). The appearance of bands at 1170 and 1090 cm⁻¹ during the hydrogenation of formic acid on our catalysts (Fig. 7) and at 1160 and 1055 cm⁻¹ during the hydrogenation of methanol (Fig. 8) is consistent with the participation of methoxy groups in the formation of methane from formate species. The methoxy species could be further hydrogenated by Zr–H species on the support to give methane gas and regenerate the OH group (Fig. 9). Our proposal implies a bifunctional character of the catalysts, with the support providing sites for CO₂ activation and the nickel facilitating the adsorption and dissociation of hydrogen.

From our data, we cannot rule out other possibilities for the transport of hydrogen on the catalyst besides a spillover process from the Ni particles to the support. It is possible, for example, that

the CO₂-derived surface species are on sites of the support at the periphery of the Ni particles, where they would react with hydrogen. Others [17,20,60,61] have proposed that the metal-support interface might be important in determining the activity of supported metal catalysts for CO₂ methanation. In the lack of direct physical evidence of the exact location of the CO₂-derived surface species on the support (e.g., far away from the supported Ni particles, in their vicinity or at the metal-support interface) any proposal for the specific way in which the species are hydrogenated is speculative in some extent and more research is necessary to address this issue.

4. Conclusions

We investigated the adsorption of CO₂ and its methanation on samples of ZrO₂-supported Ni. Our results indicate that the samples are active at temperatures above 250 °C and IR spectra characterizing the functioning catalysts allowed identification of surface species that participate in the reaction. Specifically, our data indicate that formate species bonded to sites on the support (resulting from the hydrogenation of bicarbonate species) were intermediates in the formation of methane, consistent with previous proposals for the CO₂ methanation on samples similar to ours [13,14,24]. Separate hydrogenation experiments of formic acid and methanol allowed us to propose that methoxy species are also involved in the catalysis. No nickel carbonyl species were identified under reaction conditions, in contrast with other proposals [21–23] in which it has been suggested that CO is a reaction intermediate. Our data are indicative of a bifunctional character of the ZrO₂-supported Ni catalysts for CO₂ methanation, with the support providing sites for CO₂ activation and the Ni particles acting as sites for H₂ adsorption and dissociation.

Acknowledgments

We acknowledge the Brazilian Synchrotron Light National Laboratory (LNLS) for financial support and the staff of beamline D04-XAFS1 for assisting with the XANES measurements. This research was supported by the Consejo Nacional de Ciencia y Tecnología (CB-2013 219892).

Appendix A. Supplementary data

Supplementary data associated with this article can be found, in the online version, at <http://dx.doi.org/10.1016/j.apcatb.2017.06.063>.

References

- [1] W. Wang, S.P. Wang, X.B. Ma, J.L. Gong, *Chem. Soc. Rev.* 40 (2011) 3703–3727.
- [2] S. Scire, E.C. Crisafulli, R. Maggiore, S. Mini, O.S. Galvagno, *Catal. Lett.* 51 (1998) 41–45.
- [3] M. Marwood, R. Doepper, M. Prairie, A. Renken, *Chem. Eng. Sci.* 49 (1994) 4801–4809.
- [4] J. Weigel, R.A. Koeppel, A. Baiker, A. Wokaun, *Langmuir* 12 (1996) 5319–5329.
- [5] X. Liu, G. Lu, Z. Yan, J. Beltramini, *Ind. Eng. Chem. Res.* (2003) 6518–6530.
- [6] H. Kusama, K. Okabe, K. Sayama, H. Arakawa, *Catal. Today* 28 (1996) 261–266.
- [7] H. Kusama, K. Okabe, K. Sayama, H. Arakawa, *Energy* 22 (1997) 343–348.
- [8] X. An, Y.-Z. Zuo, Q. Zhang, D. Wang, J.-F. Wang, *Ind. Eng. Chem. Res.* 47 (2008) 6547–6554.
- [9] S. Wang, D. Sen Mao, X.M. Guo, G.Z. Lu, *Wuli Huaxue Xuebao/Acta Phys.-Chim. Sin.* 27 (2011) 2651–2658.
- [10] D. Preti, C. Resta, S. Squarcialupi, G. Fachinetti, *Angew. Chem. Int. Ed.* 50 (2011) 12551–12554.
- [11] J.C. Tsai, K.M. Nicholas, *J. Am. Chem. Soc.* 114 (1992) 5117–5124.
- [12] P. Sabatier, J.B. Senderens, *Acad. Sci.* 134 (1902) 514–516.
- [13] P.A.U. Aldana, F. Ocampo, K. Kobl, B. Louis, F. Thibault-Starzyk, M. Daturi, P. Bazin, S. Thomas, A.C. Roger, *Catal. Today* 215 (2013) 201–207.
- [14] Q. Pan, J. Peng, S.S. Wang, S.S. Wang, *Catal. Sci. Technol.* 4 (2014) 502–509.
- [15] M.R. Prairie, A. Renken, J.G. Highfield, K. Ravindranathan Thampi, M. Grätzel, *J. Catal.* 129 (1991) 130–144.

- [16] S. Sharma, Z. Hu, P. Zhang, E.W. McFarland, H. Metiu, *J. Catal.* **278** (2011) 297–309.
- [17] A. Beuls, C. Swalus, M. Jacquemin, G. Heyen, A. Karelavic, P. Ruiz, *Appl. Catal. B Environ.* **113–114** (2012) 2–10.
- [18] I.A. Fisher, A.T. Bell, *J. Catal.* **162** (1996) 54–65.
- [19] A. Erdöhelyi, M. Pásztor, F. Solymosi, *J. Catal.* **98** (1986) 166–177.
- [20] X. Wang, H. Shi, J.H. Kwak, J. Szanyi, *ACS Catal.* **5** (2015) 6337–6349.
- [21] S. ichiro Fujita, M. Nakamura, T. Doi, N. Takezawa, *Appl. Catal. A Gen.* **104** (1993) 87–100.
- [22] A. Westermann, B. Azambre, M.C. Bacariza, I. Graça, M.F. Ribeiro, J.M. Lopes, C. Henriques, *Appl. Catal. B Environ.* **174–175** (2015) 120–125.
- [23] M.A.A. Aziz, A.A. Jalil, S. Triwahyono, S.M. Sidik, *Appl. Catal. A Gen.* **486** (2014) 115–122.
- [24] J. Ashok, M.L. Ang, S. Kawi, *Catal. Today* **281** (2017) 304–311.
- [25] R. Srinivasan, B.H. Davis, *Catal. Lett.* **14** (1992) 165–170.
- [26] B. Ravell, M. Newville, *Phys. Scr.* **T115** (2005) 1007–1010.
- [27] H.G. Li, M. Rivallan, F. Thibault-Starzyk, A. Travert, F.C. Meunier, *Phys. Chem. Chem. Phys.* **15** (2013) 7321–7327.
- [28] T. Suzuki-Muresan, P. Deniard, E. Gautron, V. Petíček, S. Jobic, B. Grambow, *J. Appl. Crystallogr.* **43** (2010) 1092–1099.
- [29] S.E. Collins, M. a Baltanás, A.L. Bonivardi, *J. Phys. Chem. B* **110** (2006) 5498–5507.
- [30] M. Daturi, C. Binet, J.C. Lavalley, G. Blanchard, *Surf. Interface Anal.* **30** (2000) 273–277.
- [31] H. Takano, Y. Kiriha, K. Izumiya, N. Kumagai, H. Habazaki, K. Hashimoto, *Appl. Surf. Sci.* **388** (2016) 653–663.
- [32] Spectra of the supported Ni sample also include a small shoulder at 1534 cm^{-1} , which could be indicative of the $\nu_a(\text{CO}_3)$ vibration mode of bidentate carbonate species.
- [33] G. Busca, J. Lamotte, J. Lavalley, V. Lorenzelli, C. Erba, *J. Am. Chem. Soc.* **109** (1987) 5197–5202.
- [34] The frequency of the $\nu_a(\text{CO}_2)$ vibration mode at 1570 cm^{-1} is consistent with the presence of bidentate formate species [35]. The $\nu_a(\text{CO}_2)$ vibration mode of monodentate species appears at higher wavenumbers [36, 37].
- [35] H. Tsuneko, K. Teramura, T. Shishido, T. Tanaka, *J. Phys. Chem.* **114** (2010) 8892–8898.
- [36] T. Shido, K. Asakura, Y. Iwasawa, *J. Catal.* **122** (1990) 55–67.
- [37] S.E. Collins, M.A. Baltanás, A.L. Bonivardi, *J. Catal.* **226** (2004) 410–421.
- [38] J. Kondo, H. Abe, Y. Sakata, K.-I. Maruya, K. Domen, T. Onishi, *J. Chem. Soc. Faraday Trans. 1 Phys. Chem. Condens. Phases* **84** (1988) 511–519.
- [39] The absence of bands at 1380 and 1360 cm^{-1} on IR spectra of bare support could be due to the lower amount of adsorbed formate species on the ZrO_2 with respect to those that were formed on the ZrO_2 -supported Ni sample.
- [40] C. Schild, A. Wokaun, A. Baiker, *Fresenius J. Anal. Chem.* **341** (1991) 395–401.
- [41] Spectra of both samples also show the appearance of a shoulder at approximately 1446 cm^{-1} , which could be assigned to the $\nu(\text{CO})$ vibration mode of surface ionic carbonate species [31,42].
- [42] D. Bianchi, T. Chafik, M. Khalfallah, S.J. Teichner, *Appl. Catal. A Gen.* **105** (1993) 223–249.
- [43] G. Garbarino, D. Bellotti, E. Finocchio, L. Magistri, G. Busca, *Catal. Today* **277** (2016) 21–28.
- [44] T. Kecskés, J. Raskó, J. Kiss, *Appl. Catal. A Gen.* **268** (2004) 9–16.
- [45] I.D. Reva, A.M. Plokhotnichenko, E.D. Radchenko, G.G. Sheina, Y.P. Blagoi, *Spectrochim. Acta Part A Mol. Spectrosc.* **50** (1994) 1107–1111.
- [46] L. Ojamäe, C. Aulin, H. Pedersen, P.O. Käll, *J. Colloid Interface Sci.* **296** (2006) 71–78.
- [47] K. Taek Jung, A.T. Bell, *J. Catal.* **204** (2001) 339–347.
- [48] C. Binet, M. Daturi, *Catal. Today* **70** (2001) 155–167.
- [49] E. Finocchio, M. Daturi, C. Binet, J.C. Lavalley, G. Blanchard, *Catal. Today* **52** (1999) 53–63.
- [50] G.J. Millar, C.H. Rochester, K.C. Waugh, *J. Catal.* **142** (1993) 263–273.
- [51] For this experiment, the fragment at $m/e = 16$ was used instead of that at $m/e = 15$, because the latter is also a fragment of methanol.
- [52] D. Bianchi, T. Chafik, M. Khalfallah, S.J. Teichner, *Appl. Catal. A Gen.* **123** (1995) 89–110.
- [53] K.T. Jung, A.T. Bell, *Top. Catal.* **20** (2002) 97–105.
- [54] The frequencies of both bands are different from those observed during the formic acid hydrogenation (at 1170 and 1090 cm^{-1} , Fig. 6B). The difference could be attributed to the fact that part of the Zr^{4+} surface sites were reduced to Zr^{3+} during the formic acid hydrogenation at high temperatures.
- [55] E.K. Plyler, *J. Res. Natl. Bur. Stand.* **48** (1952) 281–286.
- [56] M. Falk, E. Whalley, *J. Chem. Phys.* **34** (1961) 1554–1568.
- [57] R. Kramer, M. Andre, *J. Catal.* **58** (1979) 287–295.
- [58] D.L. Hoang, H. Berndt, H. Lieske, *Catal. Lett.* **31** (1995) 165–172.
- [59] P. Bothra, G. Periyasamy, S.K. Pati, *Phys. Chem. Chem. Phys.* **15** (2013) 5701–5706.
- [60] M. Marwood, R. Doepper, A. Renken, *Appl. Catal. A* **151** (1997) 223–246.
- [61] P. Panagiotopoulou, D.I. Kondarides, X.E. Verykios, *J. Phys. Chem. C* **115** (2011) 1220–1230.